Electronic Supplementary Material (ESI) for Nanoscale.

Nanopillar modified high-sensitivity asymmetric Graphene-GaN photodetector

Chang Liu,[a,b†] Xiaodong Li,[a,b†] Tiangui Hu,[a,b] Wenkai Zhu,[a] Faguang Yan,[a] Tiesheng Wu,[c] Kaiyou Wang,[a] Lixia Zhao,[a,b,d*]

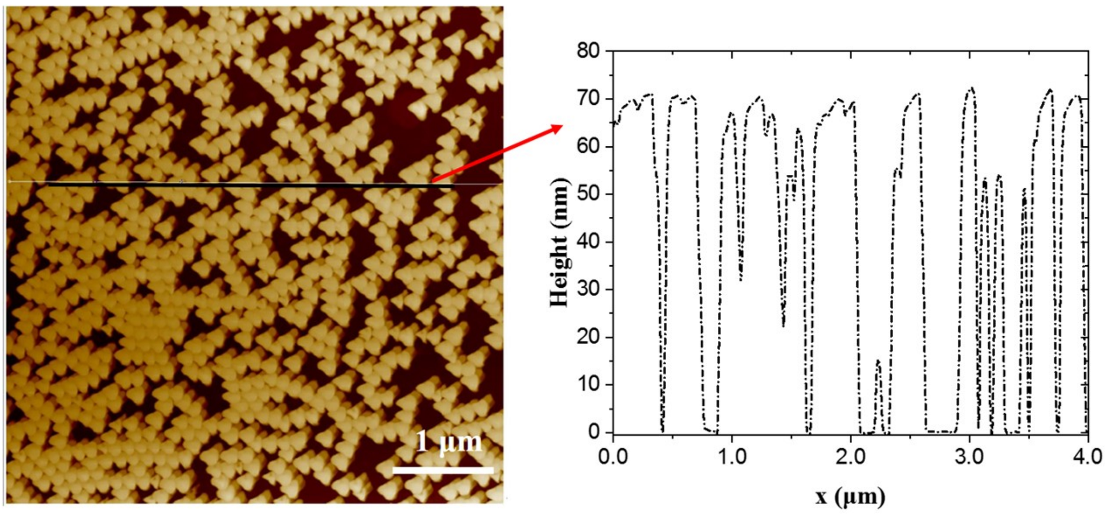

Fig. S1. AFM image of the nanopillars.

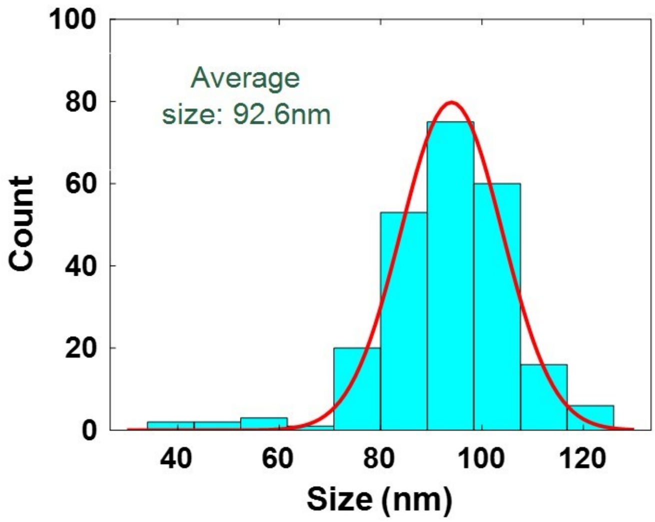

Fig. S2. Diameter distribution of the etched nanopillars.

Fig. S2 shows the diameter distribution of the nanopillars. The average diameter of nanopillars is 92.6nm, diverging from theoretical design (80 nm). However, the difference will only influence a little since the light absorption is not very sensitive to the diameter of the nanopillars as shown in Fig. 1b.

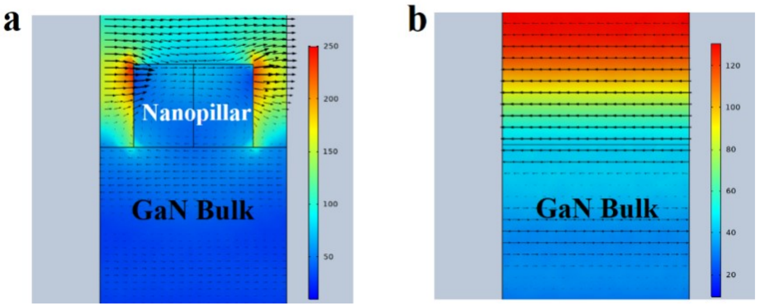

Fig. S3. a and b are the FEM simulated electric field distribution and electric vector for a unit cell of GaN nanopillar and GaN flat film, respectively.

Fig. S3 is the simulation result of the electric field distributions for the GaN film with and without nanopillars. Enhanced and localized field can be observed at the top of the nanopillars from Fig. S2a.

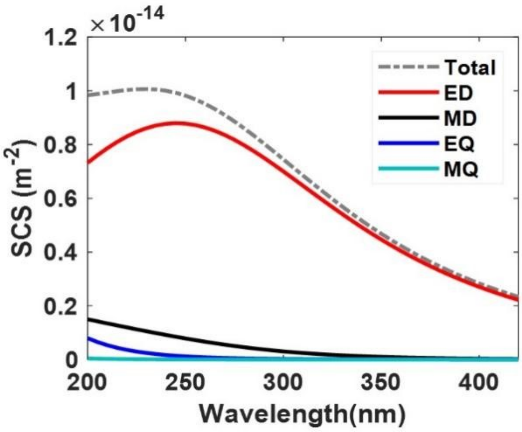

Fig. S4. EME simulated electromagnetic modes, characterized by the intensity of the scattering cross section (SCS) when the pillar size is D=80nm and H=60nm. ED, MD, EQ, and MQ represent electric dipole, magnetic dipole, electric quadrupole, and magnetic quadrupole, respectively.

The physical explanation of the nanopillar field enhancement can be understood using a numerical electromagnetic multipole expansion (EME) result, which shows that a dominant electric dipole (ED) mode arises in the GaN nanopillars.

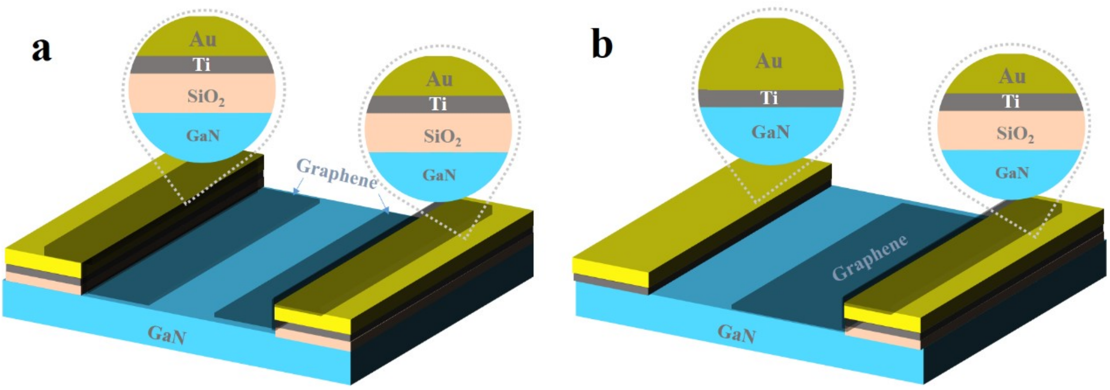

Fig. S5. Schematics of the control PDs, PD1 (a) and PD2 (b).

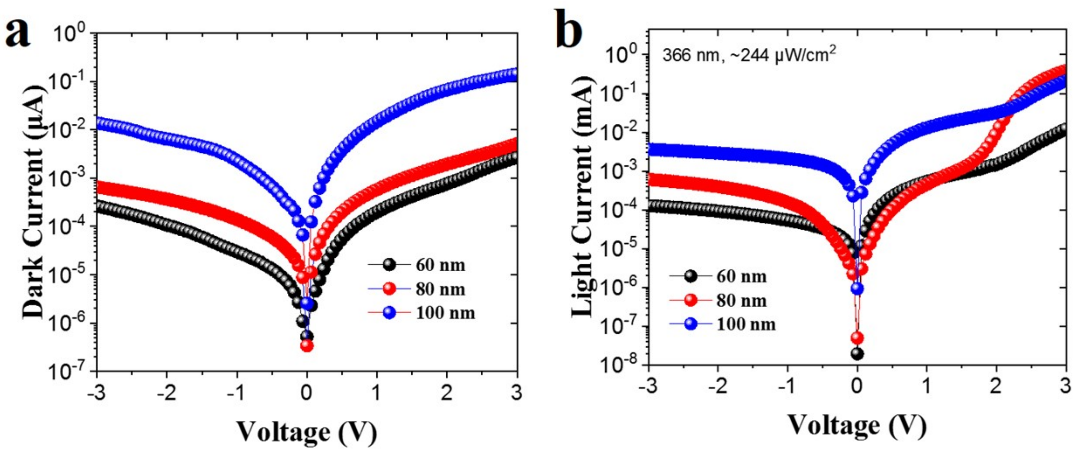

Fig. S6. a. Dark current and b. light current for the proposed PD with different pillar diameters.

The dark and light currents of the PDs with different pillar diameter have been plotted in Fig. S6. In Fig. S6a, the dark currents decrease with the shrinking of nanopillar diameter, because the graphene-nanopillar contact area reduces. Instead, in Fig. S6b, the light current basically increases with the increment of nanopillar diameter due to the enlarged graphene-nanopillar contact area. At +3 V bias, the corresponding specific detectivity of the PDs are 2.51×10^{14}, 5.8×10^{15} and 5.97×10^{14} Jones, respectively, with the increment of pillar diameter. Therefore, the PD with a moderate pillar diameter shows the best detecting performance due to its relatively lower dark current and larger light current.

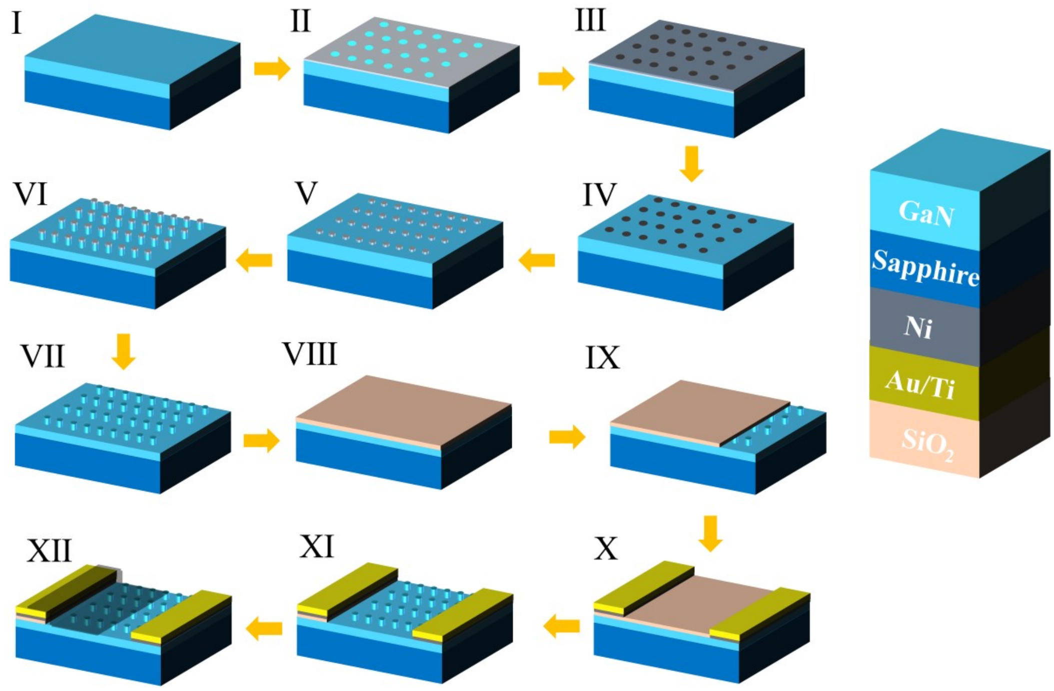

Fig. S7. Fabrication processes of the proposed PD.

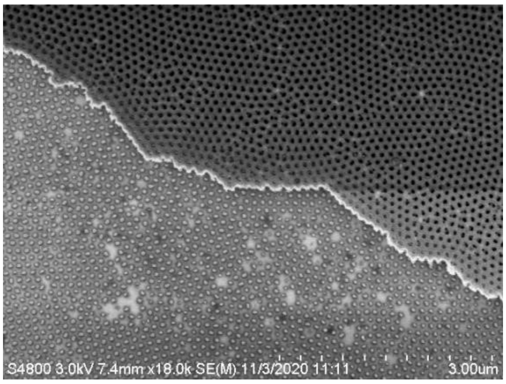

Fig. S8. SEM image of the GaN/AAO film deposited with 100nm Ni. A part of AAO film is removed by an adhesive tape to expose the beneath Ni array.

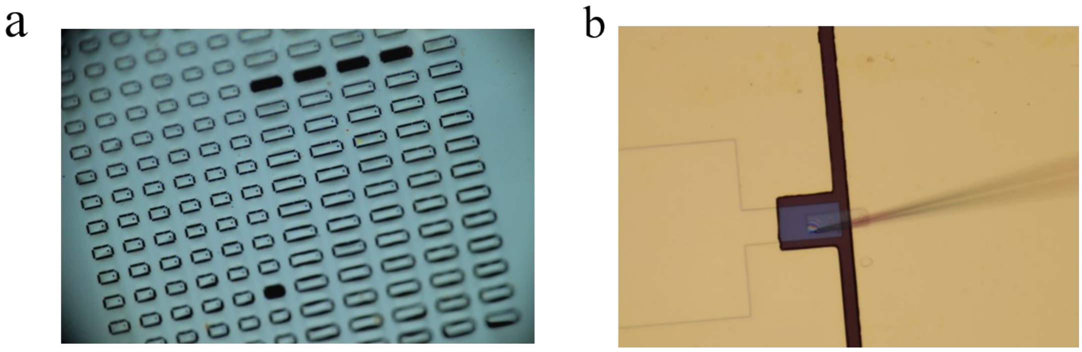

Fig. S9. a. Fabricated PMMA/graphene stamps array. b. Transferring graphene stamp onto the fabricated PD using a site-specific transfer-printing technique.